**First European Conference on Earthquake Engineering and Seismology**
(a joint event of the 13th ECEE & 30th General Assembly of the ESC)
**Geneva, Switzerland, 3-8 September 2006**
**Paper Number: 398**

# DISPERSION REDUCTION OF SEISMIC NONLINEAR RESPONSES OF A 3 STORIES ASYMMETRIC REINFORCED CONCRETE FRAME

**A. Azarbakht [1] , M. Ghafory Ashtiany [2] and M. Dolšek [3]**

## SUMMARY

Performance-based design method which enables designers to evaluate various performance levels of a structure for a given hazard level, consists of four steps: hazard analysis, structural analysis, damage assessment and loss estimation. The structural analysis responses are formulated by statistical analysis of the results of the set of non-linear time-history analyses of typical structure for the expected earthquakes. Although mean inelastic displacement ratios are very important, it is equally important to quantify its scattering and dispersion which usually display large record-to-record variability. For a given level of confidence, it is desirable to find an efficient method which can reduce the dispersion in the results with using fewer records.

This paper proposes a method for dispersion reduction of nonlinear seismic response resulting to more reliable loss estimation. The method has been applied on a 3 stories asymmetric reinforced concrete structure. The results of a comprehensive statistical study of aleatory uncertainty distribution in structural response are presented. These uncertainties are computed for different levels of strong motions representing the seismic characteristics of a predefined scenario. The study is based on a set of time histories recorded on near-field region. Inelastic displacement ratios associated with the median values are presented and special emphasis is given to the dispersion of responses. Dispersion of the responses is monitored with emphasizing on "scaling parameters", "level of ground shaking" and "damage measure".

## 1. INTRODUCTION

In the evolving field of performance-base earthquake engineering, designers and owners are motivated to fulfill predetermined performance levels or objectives. The existing performance base design frameworks have mainly addressed the probabilistic evaluation of seismic hazards [FEMA-273, VISION 2000 and SEAOC 1995]. The resulting performance levels were based on deterministic estimates of structural performance. The recent SAC Steel Project [FEMA, 2000] provided a new probabilistic extension to the performance-based earthquake engineering (PBEE), enabling simultaneous consideration of uncertainties in both demand and capacity.

A performance-based design method enables designers to evaluate a systematic performance levels for a structure in a given hazard level environment. One component of this framework is a probabilistic seismic demand model. A probabilistic seismic demand model relates the ground motion "Intensity Measures" (IMs) to the structural "Demand Measures" (DMs). It is formulated by statistical analysis of the results of a set of non-linear time-history analyses of typical structures under expected earthquake in the urban region. A recent method that has been developed to meet these needs is "Incremental Dynamic Analysis" (IDA) [Vamvatsikos and Cornell, 2002].

[1] PhD Student, IIEES, Tehran, I.R. Iran. Email: azarbakht@iiees.ac.ir
[2] Professor, President of IIEES, Tehran, I.R. Iran. Email : ashtiany@iiees.ac.ir
[3] Assistant Professor, Faculty of Civil and Geodetic Engineering, University of Ljubljana, Slovenia. Email: mdolsek@ikpir.fgg.uni-lj.si

IDA is a method which offers seismic demand and capacity prediction capability by using a series of nonlinear dynamic analyses under scaled ground motion records. To apply the method, one needs to choose a compatible ground motion IM and a representative DM. In addition, proper interpolation and summarization techniques for multiple records need to be employed, providing the means for estimating the probability distribution of demand given intensity. Limit-states, such as dynamic global system instability, can be naturally defined in the context of IDA, which allows the calculation of the annual rates of exceedance. It can be quantifying dynamic instability to numerical instability in the prediction of collapse. Clearly the non-convergence of the time-integration scheme is perhaps the safest and maybe the only numerical equivalent of the actual phenomenon dynamic collapse. But as in all models, this one can suffer from the quality of the numerical code, the number of integration steps and even the round-off error.

IDA curves display large variation from one event to another one. Sometimes the ratio of largest to smallest observation is a factor of more than ten [Cornell et. al., 1998]. The variation of IDA curves is function of several parameters, e.g. IM, DM, selected scenario earthquake and characteristics of structure as shown in Figures 1 and 2 for thirty-one scenario earthquake. Actually scaled records with a unique spectral value at the fundamental period of a single degree of freedom, "SDOF", system which remains elastic during the excitation will produce responses with zero dispersion. Beyond SDOF (contribution of higher modes) or entering the inelastic region, the structural response is not the same for different earthquakes and hence dispersion will occur. This dispersion may have significant effects in the result. In this paper focus is on IM which is connector between earthquakes and structural responses (IM, e.g. peak ground acceleration, PGA, or the 5%-damped first-mode spectral acceleration $S_a(T_1,5\%)$). Some IMs are more efficient than others, better capturing and illustrating the differences from record to record, thus bringing the results from all records closer together.

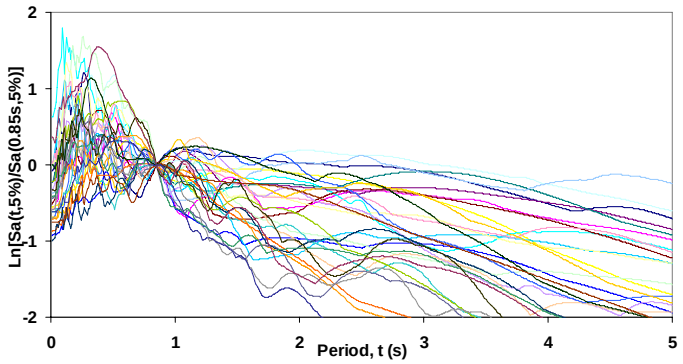


**Figure 1: The 5%-damped elastic acceleration spectra for thirty one scenario records, normalized to the spectral acceleration at period of 0.85 second.**

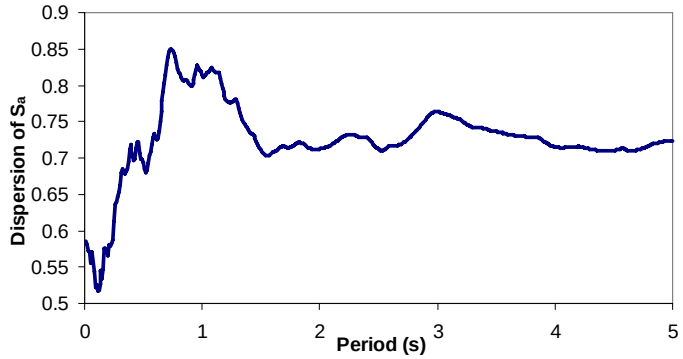


**Figure 2: Standard deviation of the natural log of the spectral acceleration $S_a$, varies across period for thirty one unscaled scenario records.**

Why finding a better IM is important? There is a clear computational advantage in selection of influenced parameters, before the IDAs are performed. By reducing the dispersion in the IDA curves there is fewer records to achieve a given confidence. Typically a reduction of the dispersion by a factor of two means that there are four times fewer records to gain the same confidence [Vamvatsikos and Cornell, 2004].

Many studies have shown that the elastic spectral shape can be a useful tool in determining an improved IM. Shome and Cornell [1999], found that the inclusion of spectral values at the second mode period ($T_2$) and at the

third-mode ($T_3$), namely $S_a(T_2,5\%)$ and $S_a(T_3,5\%)$, significantly improved the efficiency of $S_a(T_1,5\%)$ for tall buildings. Carballo and Cornell [2000], observed substantially variability reduction in the responses when spectral shape information was included by compatibilizing a suite of records to their median elastic spectrum. In addition, Mehanny and Deierlein [2000] and Cordova et al [2000], observed an improvement in the efficiency of $S_a(T_1,5\%)$ when an extra period, longer than the first-mode was included by employing an IM of the form $S_a(T_1,5\%)^{1-\beta} S_a(cT_1,5\%)^{\beta}$ with the suggested values of $\beta = 0.5,\ c = 2$. Based on these results, some of the above mentioned methods applied to a three stories asymmetric reinforced concrete frame building with a fundamental period of 0.85 second to reduce the dispersion in IDA curves.

## 2. TEST STRUCTURE AND MATHEMATICAL MODEL

The structure used in the example is three storeys asymmetric reinforce concrete frame tested pseudo-dynamically in full scale within the European research project SPEAR (Seismic performance assessment and rehabilitation of existing buildings) [Negro, Mola, Molina, Magonette, 2004].

The elevation and the plan view as well as the typical reinforcement in beam and columns of the "SPEAR" building are presented in Figure 3. The storey height, measured from top to top of the slab, is 3.0 m. The dimensions of most of columns are 25/25 cm. The only exception is column C6 which dimensions are 25/75 cm. The depth of beams is 25 cm and the height of beams, taking into account also the thickness of the slab (15 cm), is 50 cm.

The vertical reinforcement in the square columns is represented by four 12 mm smooth bars with the 8 mm stirrups at 25 cm distances. The strong column was reinforced with the eight 12 mm bars, four at the edges, two on the each long side of the column and one on the short side of the column (Figure 3). Vertical bars in the columns are lap spliced over 40 cm above the floor level including the bottom storey. Spliced bars have a 180° hooks. The same stirrups as for the square columns were used also for the strong column C6. Note that the stirrups do not continue in the joints, that they are closed with 90° hooks and that the clear cover of stirrups is 1.5 cm. The typical longitudinal reinforcement of beam consists of two 12 mm bars at the top and at the bottom, with insufficient anchorage length at the joints. Other longitudinal reinforcement is bent up towards the supports and later in the joint bent down into the joint core with the 180° hooks at the end. Stirrups of the beams are constructed with the 8 mm bars. More details regarding reinforcement are given by Fardis [2002].

The structure was designed only to gravity loads. Additional to the self weight of structure the gravity load on slabs due to finishing (0.5 kN/m2) and for live load (2.0 kN/m2) were assumed in the design process [Fardis, 2002].

The mean compressive strength of the concrete amounted to 25 MPa, while the mean strength of steel was rather high and amounted to 459 MPa for the 12 mm bars and 377 MPa for the 20 mm bars, which are used in some beams.

So called post-test mathematical model [Dolšek and Fajfar, 2005] created in the OpenSees program [PEER, 1999] was employed for analyses performed in this study. The mathematical model consists of beam and column elements for which the flexural behaviour was modelled by one-component lumped plasticity elements, composed of an elastic beam and two inelastic rotational hinges (defined by the moment-rotation relationship). The element formulation was based on the assumption of an inflexion point at the midpoint of the element. For beams, the plastic hinge was used for major axis bending only. For columns, two independent plastic hinges for bending about the two principal axes were used. The moment-rotation envelope for inelastic rotational hinges was determined based on axial force from vertical load and zero axial force for hinges in columns and beams, respectively. The maximum storey drift time histories observed in the experiment are presented in Figure 4 and compared to the calculated results. A more detailed explanation of the model and comparison with experimental results can be found in [Dolšek and Fajfar, 2005]. The input files of the mathematical model of the SPEAR building are available at www.ikpir.com\projects\spear.

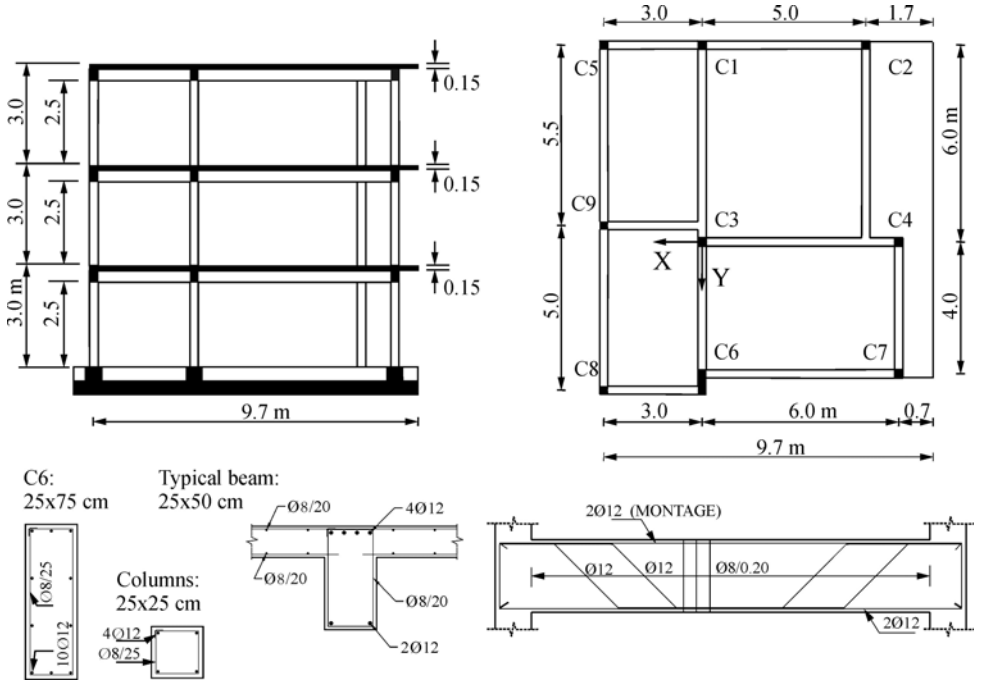


**Figure 3: The elevation, the plan view and the typical reinforcement of the SPEAR building.**

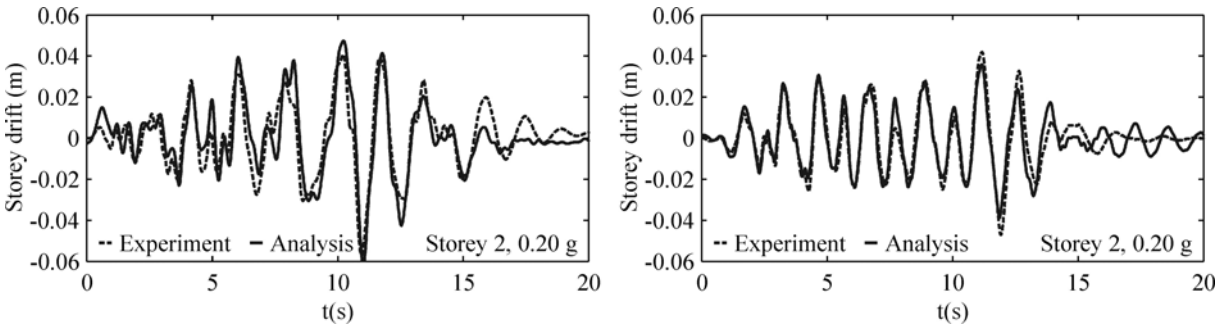


**Figure 4: Comparison between calculated and test results for a second storey drift at mass center and for a ground motion with PGA = 0.2 g.**

## 3. IDA AND DISPERSION MEASURE EVALUATION

Although summarized (e.g. median or mean) IDA curve is very important it is also important to know the scattering around the mean values, and, in particular, the quantification of dispersion in each level. A common and effective way to quantify the dispersion is through the standard deviation of the natural logarithm of the results. However this method works only until collapse appears in first IDA curve. In our study the dispersion is calculated from 16% and 50% fractile values with assuming the lognormal distribution of drifts for a given IM and vise versa. However this assumption in not valid after some collapses appears in single IDAs therefore the results for dispersion measure were calculated only to the collapse of median IDA curve. This procedure was done with two viewpoints, one for DM given a specified IM and another for IM given DM. The median IDA curves as well as 16% and 84% fractiles were calculated according to definition that $i^{th}$ point, sorted from minimum to maximum value, of N=31 values for a given seismic intensity represents 100(i-0.5)/N fractile. For example 7-th and 8-th point of N=31 points corresponds to 21% and 24% fractile. Linear interpolation was used to compute fractiles for the percent values between the discrete values of top displacement obtained from IDA analysis for a given seismic intensity. The results for summarized IDA curves and the dispersion measures are illustrated at section 5 and 6.

SPEAR building is employed for the investigation into the potential use of the different IMs. A 3D mathematical model of the building which had been prepared by Dolšek and Fajfar [2005], under "Opensees version 1.6.2.a" package, was used to performing nonlinear time histories. A set of ground motions, as described in section 3, are used to simulate a scenario earthquake. Each record component was used as an individual input in the X direction of 3D structural model and monitoring the nonlinear response. All records were appropriately scaled to cover the entire range of structural response for the building, from elastic behaviour, to inelastic region, and finally global dynamic instability. At each scaling level a non-linear dynamic analysis was performed and a single scalar was used to describe the structural response which is maximum interstory drift ratio, $\theta_{max}$, in this case.

Initial analyses were performed with peak ground acceleration (PGA), employing the scaling interval of 0.01 g, as an IM and with a post processing of the results; no future dynamic analyses are needed to change from PGA to another scalar IM. It is only required to transform each response value in the co-ordinates of the trial IMs and calculate their new dispersion. For clarify of exposition, assume that PGA and spectral acceleration at the fundamental period of structure for $i^{th}$ unscaled record is called $PGA_i$ and $S_{ai}(T_1,5\%)$ respectively. Response of the structure at the level of $PGA$ for the $i^{th}$ record is $\theta_{max}$ which is under scaled record with a scale factor of $PGA / PGA_i$. By transforming from $PGA$ to $S_{ai}(T_1,5\%)$, it is logical that $\theta_{max}$ occurs at $(PGA / PGA_i) \times S_{ai}(T_1,5\%)$. It makes useful capabilities for analyst to produce IDAs for many other new scalar IMs without performing any new analyses.

## 4. NEAR FIELD EARTHQUAKE GROUD MOTION DATA BASE

In this study a set of 31 near-source (closest source-to-site distance, $R_{close}$, less than 16km), strike-normal ground motion components recorded under forward directivity conditions from four different earthquakes is considered. For 30 out of 31 records, the causing events have moment magnitude, $6.5 \le M_w \le 7.5$, and the last one has $M_w = 6.9$. All the ground motions were recorded on NEHRP $S_D$ or $S_C$ sites, e.g. [FEMA 368, 2001], and were uniformly processed by Walter Silva for the PEER Strong Ground Motion Database (http://peer.berkeley.edu/smcat/). The characteristics of the records are summarized in Table 1, but the interested reader can find additional details in Luco (2002).

From the 5%-damped acceleration elastic response spectra, as shown in Figure 5, the large variability implicit in this data set, that is representative of a $M_w$-$R_{close}$ of fairly limited size, illustrates an important phenomenon. For example, the PGA has more than a tenfold variation from 0.08 g to about 0.9 g and the dispersion measure of $S_a$, varies across period from 0.5 to 0.85. These values are consistent with those of modern soil attenuation relationships, e.g. [Abrahamson and Silva, 1997].

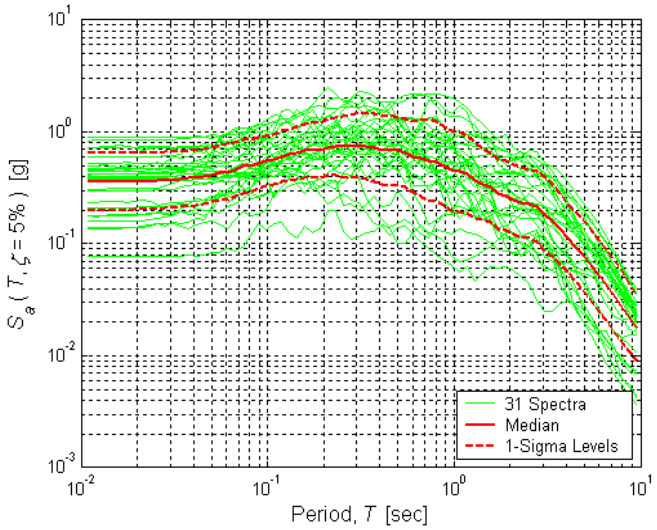


**Figure 5: 5% damped elastic response spectra for the 31 ground motions [Bazurro and Luco, 2003]**

**Table 1: Near-field ground motion earthquake records used in this study**

| Earthquake Location | Year | $M_w$ | Source Mech. | Station | $R_{close}$ (km) | PGA (%g) | $S_a(T_1,5\%)$ (%g) | $S_v(T_1,5\%)$ (m/s) | $S_d(T_1,5\%)$ (m) |
|---|---|---|---|---|---|---|---|---|---|
| (1) Imperial Valley | 1979 | 6.5 | SS | Brawley Airport | 8.5 | 0.158 | 0.173 | 0.229 | 0.031 |
| (2) | | | | EC County Center FF | 7.6 | 0.180 | 0.323 | 0.428 | 0.058 |
| (3) | | | | EC Meloland Overpass FF | 0.5 | 0.378 | 0.660 | 0.875 | 0.118 |
| (4) | | | | El Centro Array #1 | 15.5 | 0.138 | 0.073 | 0.097 | 0.013 |
| (5) | | | | El Centro Array #4 | 4.2 | 0.357 | 0.453 | 0.601 | 0.081 |
| (6) | | | | El Centro Array #5 | 1.0 | 0.375 | 0.633 | 0.840 | 0.114 |
| (7) | | | | El Centro Array #6 | 1.0 | 0.442 | 0.555 | 0.736 | 0.100 |
| (8) | | | | El Centro Array #7 | 0.6 | 0.462 | 1.171 | 1.554 | 0.210 |
| (9) | | | | El Centro Array #8 | 3.8 | 0.468 | 0.472 | 0.626 | 0.085 |
| (10) | | | | El Centro Array #10 | 8.6 | 0.176 | 0.177 | 0.235 | 0.032 |
| (11) | | | | El Centro Array #11 | 12.6 | 0.370 | 0.268 | 0.355 | 0.048 |
| (12) | | | | El Centro Differential Array | 5.3 | 0.417 | 0.423 | 0.562 | 0.076 |
| (13) | | | | Westmorland Fire Sta | 15.1 | 0.077 | 0.111 | 0.148 | 0.020 |
| (14) | | | | Parachute Test Site | 14.2 | 0.135 | 0.133 | 0.177 | 0.024 |
| (15) Superstition Hills (B) | 1987 | 6.7 | SS | El Centro Imp. Co. Cent | 13.9 | 0.308 | 0.434 | 0.576 | 0.078 |
| (16) | | | | Westmorland Fire Sta | 13.3 | 0.210 | 0.373 | 0.495 | 0.067 |
| (17) | | | | Parachute Test site | 0.7 | 0.419 | 0.837 | 1.110 | 0.150 |
| (18) Loma Prieta | 1989 | 6.9 | RV/OB | Saratoga - W Valley Coll. | 13.7 | 0.403 | 0.745 | 0.989 | 0.134 |
| (19) Northridge | 1994 | 6.7 | TH | Canyon Country - W Lost Cany | 13.0 | 0.466 | 0.580 | 0.770 | 0.104 |
| (20) | | | | Jensen Filter Plant # | 6.2 | 0.393 | 0.776 | 1.030 | 0.139 |
| (21) | | | | Newhall -Fire Sta # | 7.1 | 0.724 | 1.477 | 1.960 | 0.265 |
| (22) | | | | Rinaldi Receiving Sta # | 7.1 | 0.887 | 2.122 | 2.815 | 0.381 |
| (23) | | | | Sepulveda VA # | 8.9 | 0.722 | 1.119 | 1.486 | 0.201 |
| (24) | | | | Sun Valley - Roscoe Blvd | 12.3 | 0.298 | 0.537 | 0.712 | 0.096 |
| (25) | | | | Sylmar - Converter Sta # | 6.2 | 0.594 | 1.607 | 2.132 | 0.288 |
| (26) | | | | Sylmar - Converter Sta East # | 6.1 | 0.839 | 1.280 | 1.699 | 0.230 |
| (27) | | | | Sylmar - Olive View Med FF # | 6.4 | 0.733 | 0.735 | 0.976 | 0.132 |
| (28) | | | | Arleta - Nordhoff Fire Sta # | 9.2 | 0.237 | 0.328 | 0.435 | 0.0589 |
| (29) | | | | Newhall - W. Pico Canyon Rd. | 7.1 | 0.426 | 0.910 | 1.207 | 0.163 |
| (30) | | | | Pacoima Dam (downstr) # | 8.0 | 0.499 | 0.346 | 0.459 | 0.062 |
| (31) | | | | Pacoima Kagel Canyon # | 8.2 | 0.527 | 0.971 | 1.288 | 0.174 |

## 5. DM DISPERSION vs. GIVEN IMs

In this section dispersion of responses versus different common IMs is comprehensively examined. For this purpose PGA, $S_a(T_1,5\%)$, $S_v(T_1,5\%)$, $S_d(T_1,5\%)$, $S_a(T_1,5\%)^{0.5}S_a(2T_1,5\%)^{0.5}$, $S_v(T_1,5\%)^{0.5}S_v(2T_1,5\%)^{0.5}$ and $S_d(T_1,5\%)^{0.5}S_d(2T_1,5\%)^{0.5}$ were selected as the representative IMs and with the prescribed algorithm, which is illustrated in section 2, the dispersion of results is calculated as seen in Figures 6 to 12 respectively.

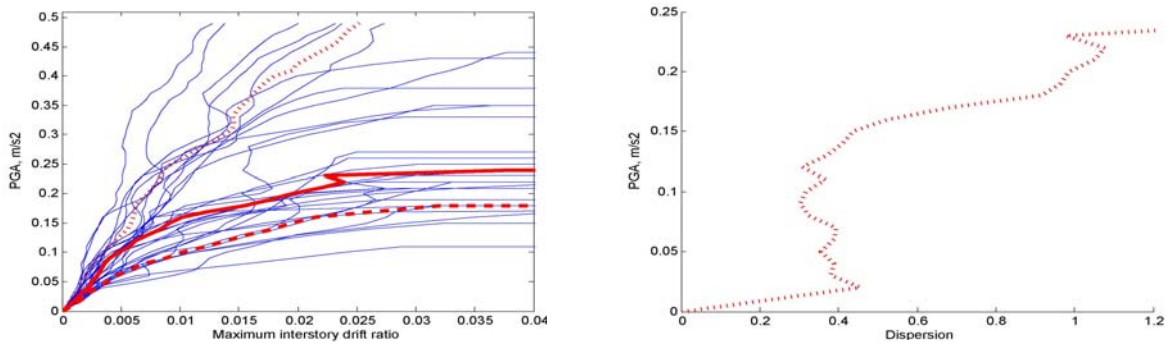


(a) (b)

**Figure 6: (a) IDA curves for the $T_1 = 0.85\,s$, SPEAR building, with median, 16% and 84% fractile curves vs. PGA, (b) IDAs dispersion vs. PGA.**

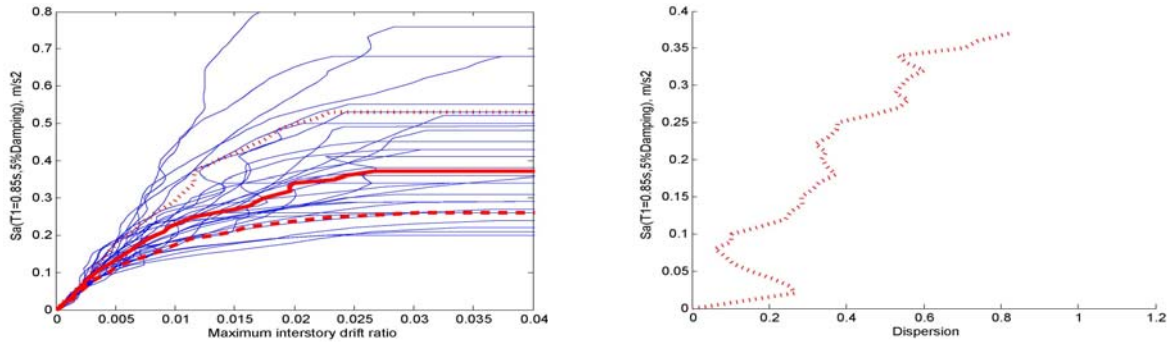


(a) (b)

**Figure 7: (a) IDA curves for the $T_1 = 0.85\,s$, SPEAR building, with median, 16% and 84% fractile curves vs. $S_a(T_1,5\%)$, (b) IDAs dispersion vs. $S_a(T_1,5\%)$**

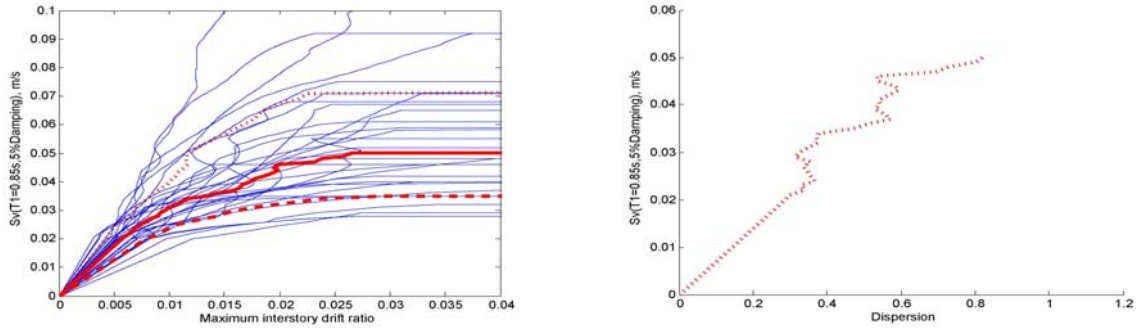


(a) (b)

**Figure 8: (a) IDA curves for the $T_1 = 0.85\,s$, SPEAR building, with median, 16% and 84% fractile curves vs. $S_v(T_1,5\%)$, (b) IDAs dispersion vs. $S_v(T_1,5\%)$**

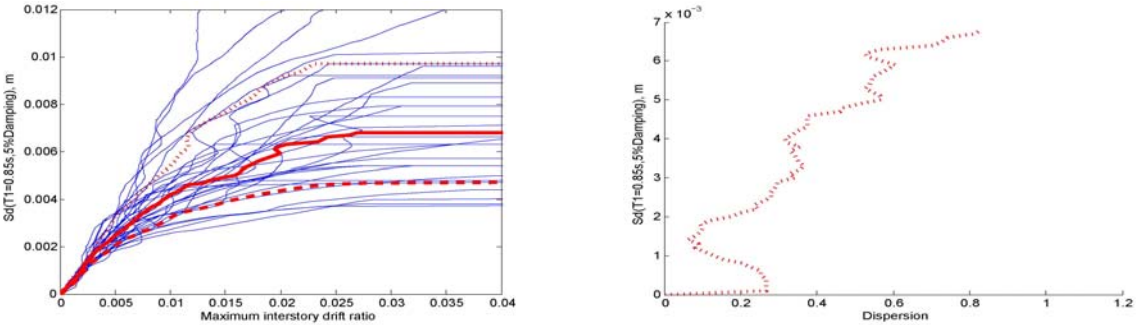


(a) (b)

**Figure 9: (a) IDA curves for the $T_1 = 0.85\,s$, SPEAR building, with median, 16% and 84% fractile curves vs. $S_d(T_1,5\%)$, (b) IDAs dispersion vs. $S_d(T_1,5\%)$**

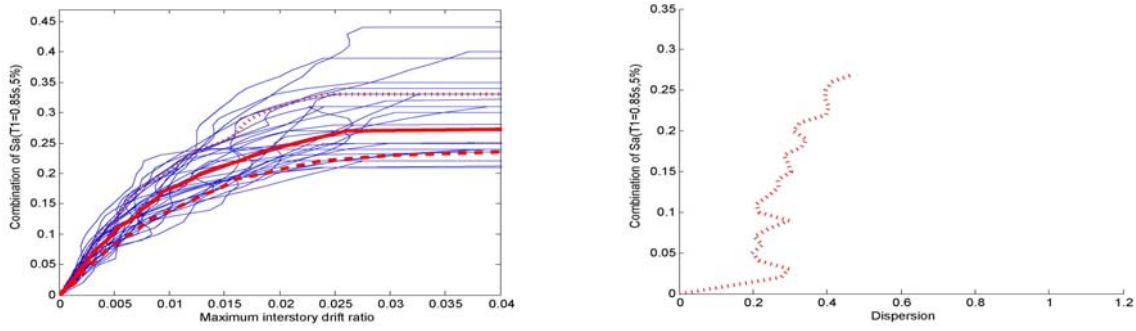


(a) (b)

**Figure 10: (a) IDA curves for the $T_1 = 0.85\,s$, SPEAR building, with median, 16% and 84% fractile curves vs. $S_a(T_1,5\%)^{0.5} S_a(2T_1,5\%)^{0.5}$, (b) IDAs dispersion vs. $S_a(T_1,5\%)^{0.5} S_a(2T_1,5\%)^{0.5}$**

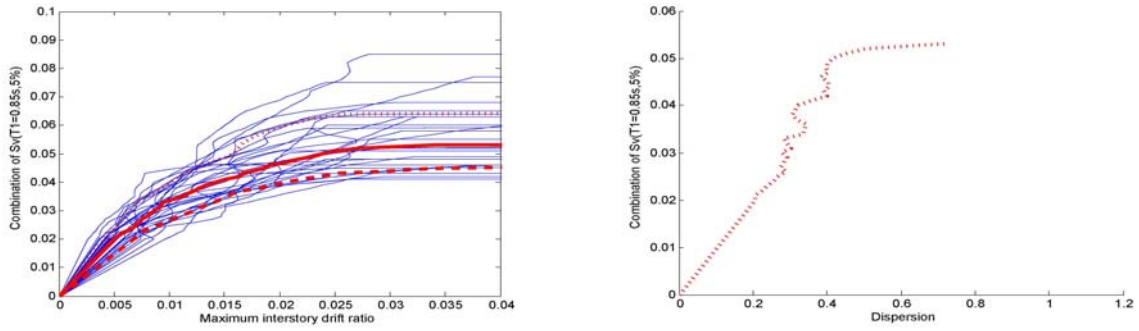


(a) (b)

**Figure 11: (a) IDA curves for the $T_1 = 0.85\,s$, SPEAR building, with median, 16% and 84% fractile curves vs. $S_v(T_1,5\%)^{0.5} S_v(2T_1,5\%)^{0.5}$, (b) IDAs dispersion vs. $S_v(T_1,5\%)^{0.5} S_v(2T_1,5\%)^{0.5}$**

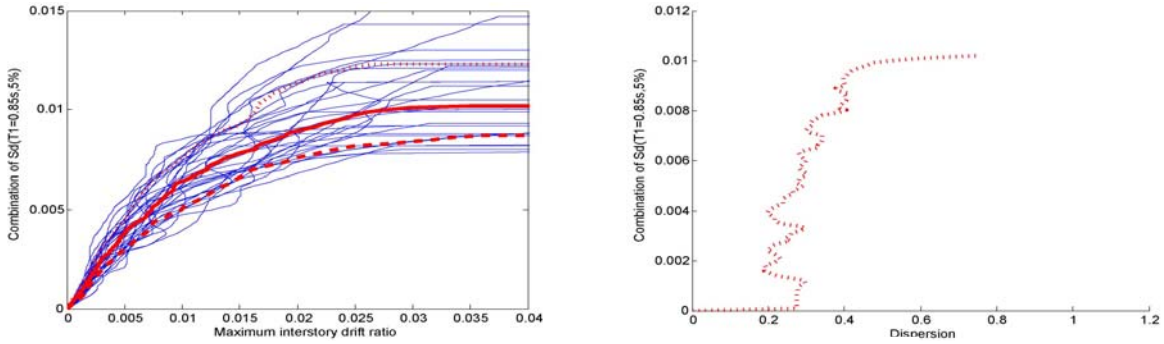


(a) (b)

**Figure 12: (a) IDA curves for the $T_1 = 0.85\,s$, SPEAR building, with median, 16% and 84% fractile curves vs. $S_d(T_1,5\%)^{0.5} S_d(2T_1,5\%)^{0.5}$, (b) IDAs dispersion vs. $S_d(T_1,5\%)^{0.5} S_d(2T_1,5\%)^{0.5}$**

According to the Figures 6 to 12, using of spectral quantities, significantly reduce the dispersion of maximum interstory drift ratio. With this reduction the dispersion remains in the range of 40% to 45% which denotes the importance of any new methods which can reduce it more. It also shows that structural dependent IMs may be more efficient than structural independent IMs. Another phenomenon which is present in these curves is the dispersion trend versus increasing the level of excitation. All Figures show an increasing in dispersion measure with increasing in the level of excitation.

## 6. IM DISPERSION vs. GIVEN DMs

In this section dispersion of IMs versus different level of DMs is examined. For this purpose three alternative IMs, including PGA, $S_a(T_1,5\%)$ and $S_a(T_1,5\%)^{0.5} S_a(2T_1,5\%)^{0.5}$, were selected. Results from other IMs are not more effective than these representatives. Results are shown in Figures 13.

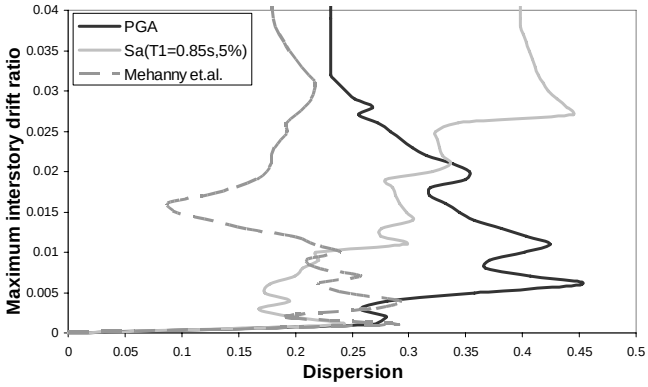


**Figure 13: Dispersion of IMs given a specified IM**

According to Figure 13, dispersion of IMs given PGA is almost greater than other alternatives. With comparing of results from other two alternatives, it is clear that for DMs smaller than 1% (low nonlinearity) $S_a(T_1,5\%)$ has lower dispersion and for DMs greater than 1% (high nonlinearity), $S_a(T_1,5\%)^{0.5}S_a(2T_1,5\%)^{0.5}$ is more effective.

## 7. CONCLUSION

Different intensity measures were employed in IDA analysis of a three storey reinforced concrete frame building with the purpose of dispersion reduction in nonlinear response. The study indicated that more efficient IMs substantially reduce the dispersion in nonlinear response. Consequently less ground motion can be used for the same efficiency of IDA analysis. The record-to-record dispersion in the results that is observed with traditional IMs can be reduced by taking advantage of elastic spectrum quantities but efficiency of different spectral quantities seems to be in the same range.

It seems that in this branch of literature, significant work remains to be done. Additional structures subjected to different set of ground motions records and employing also different methods for calculation of dispersion measure should be studied in the future to find more reliable IMs that will be both efficient and sufficient for a given structure and site. Although it was shown that more sophisticated IM can reduce record-to-record dispersion the seismic hazard curves for these IMs are not yet available. Therefore more sophisticated IMs can not yet be applied to probabilistic seismic performance analysis of structure.

## 8. ACKNOWLEDGEMENT

The authors are very grateful to Dr Walt Silva, Dr. Norman Abrahamson and Nicholas Gregor for providing and Dr Nicolas Luco for sharing us with the original records. The work greatly benefited from the comments that are received by Professor C. Allin Cornell. Comments received by Professor Ali Kave, Dr Joghatae, Dr Moghadam and Dr Ziaeefar are also very much appreciated.

## 9. REFERENCES

Abrahamson, N.A. and Silva, W.J. (1997), Empirical Response Spectra Attenuation Relations for Shallow Crustal *Earthquakes*, *Seism. Res. Lett.*, Vol. 68, No.1, pp. 94-127.

Bazzurro, P. and Cornell, C.A. (2002), Vector-valued Probabilistic Seismic Hazard Analysis (VPSHA), *Proceedings of 7th U.S. National Conference on Earthquake Engineering*, Boston, MA, July 21-25, Paper No. 61.

Carballo, J.E. and Cornell, C.A. (2000), Probabilistic Seismic Demand Analysis: Spectrum Matching and Design, *Report No. RMS-41, Department of Civil and Environmental Engineering, Reliability of Marine Structures Program, Stanford University,* Stanford, CA, July.

Cordova, PP., Deierlein, GG., Mehanny, SS. and Cornell, CA. (2000), Development of a two-parameter seismic intensity measure and probabilistic assessment procedure, *Proceeding of the 2nd U.S. Japan Workshop on Performance-Based Earthquake Engineering for Reinforced Concrete Building Structures,* Sapporo, Japan.

Cornell, C.A., Krawinkler, H. (2000), Progress and Challenges in Seismic Performance Assessment, *http://peer.berkeley.edu/news/2000spring/performance.html.*

Dolšek, M., Fajfar, P. (2005), Post-test analyses of the SPEAR test building, *University of Ljubljana, www.ikpir.com/projects/spear/*

Dolšek M., Fajfar P. (2002), Mathematical modeling of asymmetric RC frame structures based on the results of pseudo-dynamic tests, *Earthquake Engineering and Structural Dynamics* 31: 1215-1230.

Fajfar P., Dolšek M., Marušić D. and Stratan A. (2005), Pre- and post-test mathematical modelling of the SPEAR building, *Proceedings of the SPEAR International Workshop,* Ispra, April 2005.

Fardis, M.N. (2002), Design of an Irregular Buildin for the SPEAR Project – Description of the 3 – Storey Structure, *University of Patras*.

FEMA 273. (1997), NEHRP Guidelines for the Seismic Rehabilitation of Buildings, *Building Seismic Safety Council,* Washington, D.C.

Luco, N. (2002), Probabilistic Seismic Demand Analysis: SMRF Connection Fractures and Near-Source Effects, *Ph.D. Dissertation, Department of Civil and Environmental Engineering, Stanford University,* Stanford, CA.

Luco, N. and Bazzurro, P. (2003), Beyond Spectral Quantities to Improve Structural Response Estimation, *submitted to Earthquake Engineering and Structural Dynamics,* September.

Mehanny, SS. and Dierlin, GG. (2000), Modeling and asseeement of seismic performance of composit frames with reinforced concrete columns and steel beams, Report No. 136, *The John A.Blume Erathquake Engineering Center,* Stanford University, Stanford, CA.

Negro, P, Mola, E, Molina, FJ, Magonette GE, (2004), Full-scale testing of a torsionally unbalanced three-storey non-seismic RC frame. *Proceedings of the 13th World Conference on Earthquake Engineering*, paper 968.

PEER. (1999), Open System for Earthquake Engineering Simulation (OpenSees), *Pacific Earthquake Eng. Research Center,* Univ. of California, Berkeley. http://opensees.berkeley.edu/

Shome N. and Cornell, CA. (1999), Probabilistic Seismic Demand Analysis of Non-linear Structures. *Report No. RMS-35; RMS Program Stanford University,* Stanford, [http://pitch.stanford.edu/rmsweb/Theses/Nilesh Shome.pdf].

Vamvatsikos, D. and Cornell, C.A. (2005), Developing efficient scalar and vector intensity measures for IDA capacity estimation by incorporating elastic spectral shape information, *Earthquake Engineering and Structural Dynamics,* John Wiley & Sons, Ltd., New York, Vol. 34, P. 1573-1600.

Vamvatsikos, D. and Cornell, C.A. (2002), Incremental Dynamic Analysis, *Earthquake Engineering and Structural Dynamics,* Vol. 31, No. 3, John Wiley & Sons, Ltd., New York, April.